J. Math. Biol. (1992) 30: 669–691

Journal of
Mathematical
Biology

Oscillations in a model of repression with external control

Joseph M. Mahaffy[1,*], David A. Jorgensen[2,], and Robert L. Vanderheyden[3,***]**

[1] Department of Mathematical Sciences, San Diego State University, San Diego, CA 92182, USA

[2] Department of Mathematics, University of Nebraska, Lincoln, NE 68588, USA

[3] Interdisciplinary Center for Applied Mathematics, Department of Mathematics, Virginia Polytechnic Institute and State University, Blacksburg, VA 24061, USA

Received April 3, 1990; received in revised form July 6, 1991

Abstract. A mathematical model for control by repression by an extracellular substance is developed, including diffusion and time delays. The model examines how active transport of a nutrient can produce either oscillatory or stable responses depending on a variety of parameters, such as diffusivity, cell size, or nutrient concentration. The system of equations for the mathematical model is reduced to a system of delay differential equations and linear Volterra equations. After linearizing these equations and forming the limiting Volterra equations, the resulting linear system no longer has any spatial dependence. Local stability analysis of the radially symmetric model shows that the system of equations can undergo Hopf bifurcations for certain parameter values, while other ranges of the parameters guarantee asymptotic stability. One numerical study shows that the model can exhibit intracellular biochemical oscillations with increasing extracellular concentrations of the nutrient, which suggests a possible trigger mechanism for morphogenesis.

Key words: Reaction-diffusion equations – Repression – Hopf bifurcation – Delays

1 Introduction

Microorganisms extract many nutrients from their environment to maintain cell growth. When the available nutrient has a low concentration relative to intracellular concentrations, the cell must employ an active transport mechanism to acquire the nutrient. However, active transport of a substance requires a high expenditure of energy; hence, a cell which controls this process is more efficient than one which cannot. This provides a selective advantage to cells regulating active transport mechanisms. In this article a model is developed to study a system of genetic repression for controlling the transport of a nutrient across the cell membrane.

Microbial uptake of iron provides a representative example of the control system that is being studied [10, 15, 16]. In aerobic environments iron is mostly

* The work of this author was supported in part by NSF grants DMS-8603787 and DMS-8807360

** The work of this author was supported under the REU program of NSF by grant DMS-8807360

*** The work of this author was supported under the REU program of NSF by grant DMS-8807360

available as the ferric or Fe^{+++} ion which is quite insoluble (10^{-18} M at neutral pH). As an evolutionary response, bacteria have developed siderophores which have a strong affinity for Fe^{+++} ($K_m \simeq 10^{30}$ or higher) and are excreted into the environment to chelate with iron, forming a ferrienterochelin complex. In *Escherichia coli*, this complex binds to the protein FepA on the outer membrane to begin transport into the cell. Apparently, products of the *fepB* and *fepC* genes are also required to bring the complex into the cell, where ferrienterochelin esterase cleaves ferrienterochelin and releases the Fe^{+++}. The Fe^{+++} is then utilized by the cell or can complex with the constitutive protein product of the *fur* gene to produce the iron repressor protein. The iron repressor protein probably binds to the promoter region of the genes for production of siderophores and the membrane receptors or permeases, including FepA. A similar negative feedback system has been observed for the BtuB polypeptide, which is involved in the active transport of cobalamin, or vitamin B_{12}, across the outer membrane of *E. coli* [9]. The actual control mechanism for uptake of cobalamin could be either repression of transcription initiation or some posttranscriptional control.

For many nutrients microorganisms have both a low affinity transport mechanism, such as facilitated diffusion, and a high affinity transport mechanism. *E. coli* absorbs iron preferentially by passive diffusion when either ferrous ions (Fe^{++}) or ferric citrate are available in sufficient amounts [11]. Both prokaryotic and eukaryotic organisms exhibit catabolite repression of high affinity glucose transport systems when provided with a glucose rich medium [17, 19, 21]. Similarly, *E. coli* has a low affinity phosphate transport system (Pit), which is constitutive, and a high affinity, phosphate specific transport system (Pst), which is phosphate repressible [22, 23]. The model in this paper ignores the complexities involved in competing low and high affinity transport systems and focuses on the high affinity system where active transport is employed against a concentration gradient.

The mathematical model parallels a simpler repression model developed by Mahaffy and Pao [14]. It is a two compartment reaction diffusion model with three biochemical species (see Fig. 1). In the model a permease is required to transport the nutrient through the cell membrane. The nutrient diffuses through the cytoplasm to the nucleus of the cell (or a nucleoid, in the case of prokaryotes) and acts as a repressor or possibly inactivates a gene activator for the production of the mRNA necessary for production of the permease. In *E. coli*,

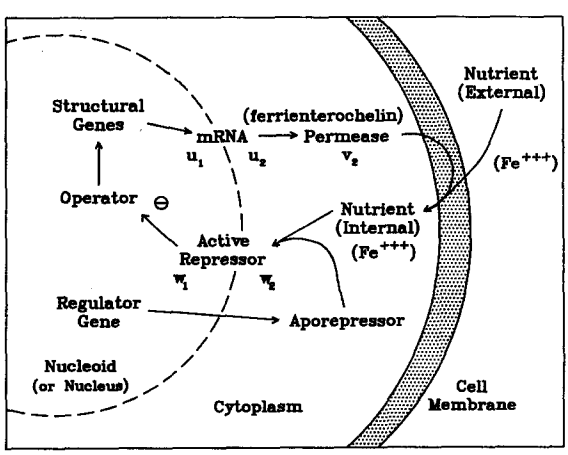

Fig. 1. A schematic for the relevant biochemical reactions in the model

the biosynthesis of iron-regulated membrane proteins [8] and the regulation of the *btuB* gene for the uptake of cobalamin [9] may have significant time lags. Thus, the model allows for time lags to occur in the steps of the biochemical reactions.

Klebba et al. [8] suggest that the regulatory scheme for iron uptake could result in oscillations in the production of the membrane proteins. Analysis of the mathematical model follows the techniques developed by Busenberg and Mahaffy [4, 5]. This scheme transforms a system of delay differential equations and partial differential equations into a system of delay differential equations and linear Volterra equations with the spatial dependence of the initial conditions exponentially damped. After this system is linearized about its equilibrium solution and the limiting Volterra equations are formed, a local analysis is performed by careful examination of the characteristic equation of this time varying system. Analysis of this characteristic equation shows that as the diffusivities become sufficiently large the local behavior of this model approaches the local behavior of a corresponding well mixed model. For certain parameter values the well mixed model is shown to exhibit oscillations; hence, the original model also develops oscillations. One result of particular significance is the decreasing stability of the intracellular concentrations of this repression model with increasing extracellular concentrations of the repressor (or precursor to the repressor). This could have important ramifications in morphogenesis, as the behavior of the cell could be altered as a result of the stability change induced by the presence of an increased concentration of some extracellular biochemical species.

Other analyses are done on the characteristic equation using theoretical and numerical studies. In the formulation of the Volterra equations, the diffusion operator is characterized, in effect, as a complicated time delay. Previous authors (e.g., [11]) have speculated that diffusion should behave in this manner, but this formulation shows it is more complicated. The numerical studies show that as the diffusivities are decreased, the model becomes less stable, as it would if the delay were increased. However, when the diffusivities are sufficiently small, Mahaffy et al. [13] have shown that the model is asymptotically stable. Mahaffy et al. [13] demonstrated a similar stability for increasing cell size. The bifurcation curves generated by the numerical analysis of the characteristic equation graphically depict all of these results.

In the next section the mathematical model is presented. In the third section the model is analyzed for high diffusivities, and the characteristic equation is formulated for further analysis by numerical computations. The fourth section contains a series of figures generated by the computer which describe how the model behaves for a range of different parameter values. The final section presents a discussion of the biological significance of these findings.

2 The mathematical model

The mathematical model has two distinct compartments as shown in Fig. 2. The first compartment labeled ω in Fig. 2 represents a nucleoid for a prokaryotic cell or a nucleus for a eukaryotic cell and is considered to be sufficiently small so that a well mixed assumption can be applied. Thus, the dynamics of the reacting biochemical species in this compartment are governed by differential equations which have no spatial component. The second compartment given by $\Omega \backslash \omega$ in Fig. 2 represents the cytoplasm of the cell. In this compartment both reactions and diffusion are considered.

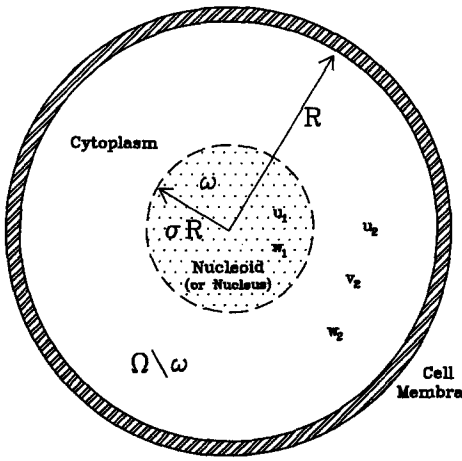

Fig. 2. Diagram for the radially symmetric cell showing the two compartments and the variables for the biochemical species

There are three biochemical species that are examined. The mRNA, which has its production controlled by a repression process, is denoted by u_i where $i = 1, 2$, depending on the compartment. In the case of a eukaryotic organism the control of the mRNA production is more likely to be the inactivation of a gene activator. Between the two compartments the mRNA is assumed to pass by a passive process which depends only on the concentration gradient of the mRNA. In the second compartment, which has spatial variation in its concentrations, the concentration gradient is determined by the concentration of the mRNA near the boundary of ω. Once in the cytoplasm, the mRNA is translated to produce a permease v_2. It is assumed that the permease is restricted to the second compartment. The permease is needed for active transport of the nutrient, w_i, across the exterior membrane, Ω, of the cell. The nutrient can then diffuse through the cytoplasm and enter the first compartment where it exerts a negative control on the production of the mRNA which produces the permease. As the processes of transcription and translation take a certain amount of time, the reactions using these processes are modeled with discrete time delays.

The reactions for a repression model have been developed by several authors [2, 6, 18, 20, 24], and so the details for the actual biochemical reactions used in this model are omitted in this discussion. A one-dimensional version of this model with an extracellular nutrient and repression has been developed and partially analyzed by Harter et al. [7]. With the assumptions made above the following model can be written:

$$
\begin{aligned}
\dot{u}_1(t) &= f(w_1(t - T_1)) - b_1 u_1(t) + a_1 \int_{\partial\omega} [u_2(x, t) - u_1(t)]\, dS_\omega, \\
\dot{w}_1(t) &= -\hat{b}_3 w_1(t) + a_3 \int_{\partial\omega} [w_2(x, t) - w_1(t)]\, dS_\omega, \\
\frac{\partial u_2}{\partial t} &= D_1 \nabla^2 u_2 - b_1 u_2, \\
\frac{\partial v_2}{\partial t} &= D_2 \nabla^2 v_2 - b_2 v_2 + g(u_2(x, t - T_2)), \\
\frac{\partial w_2}{\partial t} &= D_3 \nabla^2 w_2 - b_3 w_2,
\end{aligned}
\tag{2.1}
$$

with the boundary conditions:

$$\frac{\partial u_2(x,t)}{\partial n} = -\beta_1[u_2(x,t) - u_1(t)], \quad \text{for } x \in \partial\omega,$$

$$\frac{\partial u_2(x,t)}{\partial n} = 0, \quad \text{for } x \in \partial\Omega,$$

$$\frac{\partial v_2(x,t)}{\partial n} = 0, \quad \text{for } x \in \partial\omega \cup \partial\Omega,$$

$$\frac{\partial w_2(x,t)}{\partial n} = -\beta_3[w_2(x,t) - w_1(t)], \quad \text{for } x \in \partial\omega,$$

$$\frac{\partial w_2(x,t)}{\partial n} = kv_2(x,t), \quad \text{for } x \in \partial\Omega.$$

The kinetic constants b_i are the decay rates, and a_i are the transfer rates. The D_i are the coefficients of diffusivity, and β_i correspond to the transfer across compartment boundaries. The constant k is a parameter depending on the rate of transfer across the exterior membrane and the extracellular concentration of the nutrient. The function $f(w_1)$ incorporates the negative control of transcription by the nutrient and is assumed to have the form $1/[1 + K(w_1)^q]$. The function $g(u_2)$ represents the translation rate and is given by the linear form, c_0u_2. Note that we allow for differing decay rates, b_3 and $\hat{b_3}$, for the nutrient in the two compartments. These particular forms are derived from the biochemical kinetics using excess substrate assumptions and conservation mass properties. For more details see [1, 2, 18]. In addition, a simple time scaling and a phase shift can make $b_1 = 1$ and leave the equations with only one delay, $T = T_1 + T_2$, in the nonlinear function f.

An associated system of equations for a model where the second compartment is also well mixed can be written as follows:

$$\begin{aligned}
\dot{u}_1(t) &= f(w_1(t-T)) - u_1(t) + \alpha_1[u_2(t) - u_1(t)],\\
\dot{w}_1(t) &= -\hat{b_3}w_1(t) + \alpha_3[w_2(t) - w_1(t)],\\
\dot{u}_2(t) &= -u_2(t) + \alpha_4[u_1(t) - u_2(t)],\\
\dot{v}_2(t) &= c_0u_2(t) - b_2v_2(t),\\
\dot{w}_2(t) &= \kappa v_2(t) - b_3w_2(t) + \alpha_6[w_1(t) - w_2(t)].
\end{aligned} \tag{2.2}$$

Let $\bar{w}_1$ be the equilibrium value for $w_1(t)$ in (2.2). It can be easily shown that $\bar{w}_1$ is the unique solution to:

$$f(\bar{w}_1) = \frac{b_2[(1+\alpha_1)(1+\alpha_4) - \alpha_1\alpha_4][(\hat{b_3}+\alpha_3)(b_3+\alpha_6) - \alpha_3\alpha_6]\bar{w}_1}{c_0\kappa\alpha_3\alpha_4}.$$

From the linearization of (2.2) one finds the characteristic equation for the well mixed model, and it is given by:

$$\begin{aligned}
&(\lambda+1)(\lambda+b_2)(\lambda+1+\alpha_1+\alpha_4)[(\lambda+\hat{b_3}+\alpha_3)(\lambda+b_3+\alpha_6) - \alpha_3\alpha_6]\\
&\quad - c_0\kappa\alpha_3\alpha_4 f'(\bar{w}_1)\, e^{-\lambda T} = 0.
\end{aligned} \tag{2.3}$$

3 Analysis of the model for high diffusivities

In order to proceed with a more detailed analysis of the model presented in Sect. 2, there are several assumptions about the geometry of the cell which are used. It is assumed that the cell is modeled by two concentric spheres, where the inner sphere (the well mixed first compartment) has radius σR, $0 < \sigma < 1$, and the outer sphere (the cell membrane) has radius R. With these assumptions Eqs. (2.1) can be written as follows:

$$\begin{aligned}
\dot{u}_1(t) &= f(w_1(t-T)) - u_1(t) + \gamma_1[u_2(R\sigma, t) - u_1(t)], \\
\dot{w}_1(t) &= -\hat{b}_3 w_1(t) + \gamma_3[w_2(R\sigma, t) - w_1(t)], \\
\frac{\partial u_2}{\partial t} &= D_1 \nabla^2 u_2 - u_2, \\
\frac{\partial v_2}{\partial t} &= D_2 \nabla^2 v_2 - b_2 v_2 + c_0 u_2, \\
\frac{\partial w_2}{\partial t} &= D_3 \nabla^2 w_2 - b_3 w_2,
\end{aligned} \tag{3.1}$$

for $t > 0$ and $R\sigma < r < R$ and with the boundary conditions:

$$\begin{aligned}
&\frac{\partial u_2(R\sigma, t)}{\partial r} = \beta_1[u_2(R\sigma, t) - u_1(t)], \qquad \frac{\partial u_2(R, t)}{\partial r} = 0, \\
&\frac{\partial v_2(R\sigma, t)}{\partial r} = 0, \qquad \frac{\partial v_2(R, t)}{\partial r} = 0, \\
&\frac{\partial w_2(R\sigma, t)}{\partial r} = \beta_3[w_2(R\sigma, t) - w_1(t)], \qquad \frac{\partial w_2(R, t)}{\partial r} = k v_2(R, t),
\end{aligned}$$

where $\nabla^2 = \dfrac{1}{r^2}\dfrac{\partial}{\partial r}\left(r^2 \dfrac{\partial}{\partial r}\right)$.

For large diffusivities the qualitative behavior of system (3.1) is expected to parallel that of the well mixed model given by (2.2). A stability analysis of the linearized models shows that if the leading eigenvalues of the well mixed model have real part greater than zero, then the linearization of the reaction diffusion model with sufficiently large diffusivities has eigenvalues with real part greater than zero. Thus, instabilities in the well mixed model which result in sustained oscillations give similar instabilities in (3.1). The following theorem summarizes the comparative analysis between (2.2) and (3.1) for high diffusivities:

Theorem 3.1 *Let the parameters α_1, α_3, and κ in system* (2.2) *be fixed and fix R and σ in* (3.1). *Assume that the diffusivities D_i in* (3.1) *tend to infinity, $i = 1, 2, 3$, and consider λ such that* $\mathrm{Re}(\lambda) > \max\{-1, -b_2, -b_3\}$. *Then in the limit, the values of λ which satisfy the characteristic equation for the linearized diffusion model are equal to the solutions λ of the characteristic equation* (2.3) *for the well mixed model.*

The proof of this theorem relies on a technique of reducing the system of partial differential equations with delays to an equivalent system of delay differential equations with linear Volterra equations which depend only on the state variables at the boundary (see [4, 5]). The spatial component occurs only in an exponentially damped term depending on the initial conditions. After a

change of variables that makes the boundary conditions homogeneous, a variation of parameters technique is used with the semigroup operator coming from the linear part of the partial differential equation. The spherical geometry is necessary for the explicit calculations performed to show the existence of a Hopf bifurcation and demonstrate behavior parallel to the well mixed model; however, many of the beginning steps which reduce the system of delayed partial differential equations to a system of delay differential equations and Volterra equations with no spatial dependence can be performed in a more general setting.

The first step in the analysis of the model is to compute the steady state solution. Details of this computation are given in the Appendix. After the steady state solution is found, the system of differential equations given by (3.1) is translated about this solution for stability analysis of the zero solution. Furthermore, a change of variables is made so that the boundary conditions become homogeneous. If we let variables with an s superscript represent the steady state solution, then the following change of variables is used:

$$\begin{aligned}
U_1(t) &= u_1(t) - u_1^s, \\
W_1(t) &= w_1(t) - w_1^s, \\
U_2(r, t) &= u_2(r, t) - u_2^s(r) - U_1(t), \\
V_2(r, t) &= v_2(r, t) - v_2^s(r), \\
W_2(r, t) &= w_2(r, t) - w_2^s(r) - W_1(t) - kh(r)V_2(R, t),
\end{aligned}$$

where h must satisfy $h'(R\sigma) = \beta_3 h(R\sigma)$ and $h'(R) = 1$ to make the last two boundary conditions homogeneous. We chose $h(r) = (r - R\sigma)^2/2R(1-\sigma)$. With this change of variables (3.1) is written as follows:

$$\begin{aligned}
\dot{U}_1(t) &= \tilde{f}(W_1(t-T)) - U_1(t) + \gamma_1 U_2(R\sigma, t), \\
\dot{W}_1(t) &= -\hat{b}_3 W_1(t) + \gamma_3 W_2(R\sigma, t), \\
\frac{\partial U_2}{\partial t} &= D_1 \nabla^2 U_2 - U_2 - \tilde{f}(W_1(t-T)) - \gamma_1 U_2(r\sigma, t), \\
\frac{\partial V_2}{\partial t} &= D_2 \nabla^2 V_2 - b_2 V_2 + c_0(U_2 + U_1(t)), \\
\frac{\partial W_2}{\partial t} &= D_3 \nabla^2 W_2 - b_3 W_2 + (\hat{b}_3 - b_3) W_1 - \gamma_3 W_2(R\sigma, t) \\
&\quad + k\left[\left[\left(\frac{D_3}{r^2}\right)\frac{d}{dr}\left(r^2 \frac{dh}{dr}\right) - b_3 h\right] V_2(R, t) - h\dot{V}_2(R, t)\right],
\end{aligned} \tag{3.2}$$

for $t > 0$ and $R\sigma < r < R$ and with the boundary conditions:

$$\begin{aligned}
&\frac{\partial U_2(R\sigma, t)}{\partial r} = \beta_1 U_2(R\sigma, t), \qquad \frac{\partial U_2(R, t)}{\partial r} = 0, \\
&\frac{\partial V_2(R\sigma, t)}{\partial r} = 0, \qquad \frac{\partial V_2(R, t)}{\partial r} = 0, \\
&\frac{\partial W_2(R\sigma, t)}{\partial r} = \beta_3 W_2(R\sigma, t), \qquad \frac{\partial W_2(R, t)}{\partial r} = 0,
\end{aligned}$$

where $\tilde{f}(W_1) = f(W_1 + w_1^s) + \gamma_1 u_2^s(R\sigma) - (\gamma_1 + 1)u_1^s$.

The next step of the analysis is to examine the differential equation for $U_2(r, t)$. The technique employed parallels that of Busenberg and Mahaffy [4] in that the eigenvalues and eigenfunctions for the homogeneous part of the U_2 equation with its boundary conditions in (3.2) are found and then a variation of constants formula is applied. The eigenvalue equation from the associated Sturm–Liouville problem is given by:

$$\cot[\mu(1-\sigma)] = \frac{\mu^2\sigma + 1 + \beta_1 R\sigma}{\mu[(1-\sigma) + \beta_1 R\sigma]}. \tag{3.3}$$

The eigenfunction corresponding to eigenvalue μ is given by:

$$\phi(r) = \frac{2\sqrt{\mu}\left(\mu \cos\left[\mu\left(1-\frac{r}{R}\right)\right] - \sin\left[\mu\left(1-\frac{r}{R}\right)\right]\right)}{r\sqrt{R\sqrt{2(\mu^2+1)\mu(1-\sigma) - 4\mu R \sin^2[\mu(1-\sigma)] + (\mu^2-1)\sin[2\mu(1-\sigma)]}}}.$$

As this denominator occurs frequently in our subsequent computations, we define the following two expressions which come from the normalization of the eigenfunctions:

$$F_{\text{nor}}(\chi) = (\chi^2+1)\chi(1-\sigma) - 2\chi \sin^2[\chi(1-\sigma)] + (\chi^2-1)\sin[\chi(1-\sigma)]\cos[\chi(1-\sigma)]$$

and

$$G_{\text{nor}}(\chi, \beta) = (1-\sigma)\chi^2(1+\sigma+\sigma^2+\chi^2\sigma^2) + \beta R\sigma(\chi^2(2-\sigma)-\sigma) + \beta^2R^2\sigma^2(\chi^2(1-\sigma)-\sigma).$$

If we define $\delta_n^u = \langle 1, \phi_n \rangle = \int_{R\sigma}^{R} 1 \cdot \phi_n(r) r^2 dr$, then using some trigonometric identities we can show that:

$$\delta_n^u \phi_n(R\sigma) = \frac{2\beta_1 R\sigma^2(1+\mu_n^2)}{G_{\text{nor}}(\mu_n, \beta_1)}. \tag{3.4}$$

If we define $\alpha_n^u \equiv \langle U_{20}, \phi_n \rangle$ and $A_n \equiv 1 + \mu_n^2 D_1/R^2$, where $U_{20}(r) = U_2(r, 0)$, then the variation of constants formula gives:

$$U_2(r,t) = \sum_{n=1}^{\infty} \alpha_n^u \phi_n(r)\, e^{-A_n t} - \int_0^t \sum_{n=1}^{\infty} \delta_n^u \phi_n(r)\, e^{-A_n(t-s)}[\tilde{f}(W_1(s-T)) + \gamma_1 U_2(R\sigma, s)]\, ds.$$

If this equation is evaluated at $r = R\sigma$, then we have a linear Volterra equation in $U_2(R\sigma, t)$ which is given by:

$$U_2(R\sigma,t) = \sum_{n=1}^{\infty} \alpha_n^u \phi_n(R\sigma)\, e^{-A_n t} - \int_0^t K^u(t-s, R\sigma)[\tilde{f}(W_1(s-T)) + \gamma_1 U_2(R\sigma, s)]\, ds, \tag{3.5}$$

where $K^u(s, r) = \sum_{n=1}^{\infty} \delta_n^u \phi_n(r)\, e^{-A_n(s)}$.

A similar procedure is applied to the V_2 equation. The Sturm–Liouville problem associated with the V_2 equation has insulated boundary conditions, which implies that the first eigenvalue, $\nu_0 = 0$, has its associated (normalized) eigenfunction given by:

$$\psi_0(r) = \sqrt{\frac{3}{R^3(1-\sigma^3)}}. \tag{3.6}$$

The subsequent eigenvalues are found from the equation:

$$\cot[\nu(1-\sigma)] = \frac{\nu^2\sigma + 1}{\nu(1-\sigma)}. \tag{3.7}$$

The corresponding eigenfunctions are given by:

$$\psi(r) = \frac{\sqrt{2\nu}\left(\nu\cos\left[\nu\left(1-\frac{r}{R}\right)\right] - \sin\left[\nu\left(1-\frac{r}{R}\right)\right]\right)}{r\sqrt{R}\sqrt{F_{\text{nor}}(\nu)}}.$$

By orthogonality it is clear that $\langle 1, \psi_n \rangle = 0$, $n = 1, 2, \ldots$. If we define $\alpha_n^v \equiv \langle V_{20}, \psi_n \rangle$ and $B_n \equiv b_2 + \nu_n^2 D_2/R^2$, where $V_{20}(r) = V_2(r, 0)$, then the variation of constants formula gives:

$$\begin{aligned} V_2(r, t) = &\sum_{n=0}^{\infty} \alpha_n^v \psi_n(r)\, e^{-B_n t} + c_0 \int_0^t e^{-b_2(t-s)} U_1(s)\, ds \\ &+ c_0 \int_0^t \sum_{n=0}^{\infty} \langle U_2(\cdot, s), \psi_n(\cdot) \rangle \psi_n(r)\, e^{-B_n(t-s)}\, ds. \end{aligned} \tag{3.8}$$

The linear part of the W_2 equation is very similar to that of the U_2 equation. This implies that the eigenvalue equation and corresponding eigenfunctions are easily found and are given by:

$$\cot[\omega(1-\sigma)] = \frac{\omega^2\sigma + 1 + \beta_3 R\sigma}{\omega[(1-\sigma) + \beta_3 R\sigma]}, \tag{3.9}$$

with eigenfunction:

$$\xi(r) = \frac{\sqrt{2\omega}\left(\omega\cos\left[\omega\left(1-\frac{r}{R}\right)\right] - \sin\left[\omega\left(1-\frac{r}{R}\right)\right]\right)}{r\sqrt{R}\sqrt{F_{\text{nor}}(\omega)}}.$$

If we define $\delta_n^w \equiv \langle 1, \xi_n \rangle = \int_{R\sigma}^{R} 1 \cdot \xi_n(r) r^2\, dr$, then using some trigonometric identities we can show that:

$$\delta_n^w \xi_n(R\sigma) = \frac{2\beta_3 R\sigma^2(1+\omega_n^2)}{G_{\text{nor}}(\omega_n, \beta_3)}. \tag{3.10}$$

If we define $\alpha_n^w \equiv \langle W_{20}, \xi_n \rangle$ and $C_n \equiv b_3 + \omega_n^2 D_3/R^2$, where $W_{20}(r) = W_2(r, 0)$, then the variation of constants formula gives:

$$\begin{aligned} W_2(r, t) = &\sum_{n=1}^{\infty} \alpha_n^w \xi_n(r)\, e^{-C_n t} \\ &+ \int_0^t K^w(t-s, r)[(\hat{b_3} - b_3) W_1(s) - \gamma_3 W_2(R\sigma, s)]\, ds \\ &+ k\int_0^t \sum_{n=1}^{\infty} \langle [D_3\nabla^2 h - b_3 h], \xi_n \rangle \xi_n(r)\, e^{-C_n(t-s)} V_2(R, s)\, ds \\ &- k\int_0^t \sum_{n=1}^{\infty} \langle h, \xi_n \rangle \xi_n(r)\, e^{-C_n(t-s)} \dot{V}_2(R, s)\, ds, \end{aligned} \tag{3.11}$$

where $K^w(s, r) = \sum_{n=1}^{\infty} \delta_n^w \xi_n(r)\, e^{-C_n s}$.

If (3.8) is evaluated at R and (3.11) is evaluated at $R\sigma$, then the following system of delay differential equations and linear Volterra equations can be written:

$$
\begin{aligned}
\dot{U}_1(t) &= \tilde{f}(W_1(t-T)) - U_1(t) + \gamma_1 U_2(R\sigma, t),\\
\dot{W}_1(t) &= -\hat{b}_3 W_1(t) + \gamma_3 W_2(R\sigma, t),\\
U_2(R\sigma, t) &= \sum_{n=1}^{\infty} \alpha_n^u \phi_n(R\sigma)\, e^{-A_n t}\\
&\quad - \int_0^t K^u(t-s, R\sigma)[\tilde{f}(W_1(s-T)) + \gamma_1 U_2(R\sigma, s)]\, ds,\\
V_2(R, t) &= \sum_{n=0}^{\infty} \alpha_n^v \psi_n(R)\, e^{-B_n t} + c_0 \int_0^t e^{-b_2(t-s)} U_1(s)\, ds\\
&\quad + c_0 \int_0^t \sum_{n=0}^{\infty} \langle U_2(\cdot, s), \psi_n(\cdot)\rangle \psi_n(R)\, e^{-B_n(t-s)}\, ds,\\
W_2(R\sigma, t) &= \sum_{n=1}^{\infty} \alpha_n^w \xi_n(R\sigma)\, e^{-C_n t}\\
&\quad + \int_0^t K^w(t-s, R\sigma)[(\hat{b}_3 - b_3) W_1(s) - \gamma_3 W_2(R\sigma, s)]\, ds\\
&\quad + k \int_0^t \sum_{n=1}^{\infty} \langle [D_3 \nabla^2 h - b_3 h], \xi_n\rangle \xi_n(R\sigma)\, e^{-C_n(t-s)} V_2(R, s)\, ds\\
&\quad - k \int_0^t \sum_{n=1}^{\infty} \langle h, \xi_n\rangle \xi_n(R\sigma)\, e^{-C_n(t-s)} \dot{V}_2(R, s)\, ds.
\end{aligned}
\tag{3.12}
$$

The system of equations (3.12) only has a spatial dependence reflected in the terms α_n^u, α_n^v, and α_n^w, and these terms are exponentially damped. This suggests that standard techniques for analysis of time dependent systems are applicable.

The procedure below parallels that of Busenberg and Mahaffy [4]. The system (3.12) is first linearized, and then the limiting Volterra equations are found. As shown in Busenberg and Mahaffy [4], the terms containing α_n^u, α_n^v, and α_n^w are damped in the limit as $t \to \infty$. This allows us to write the following limiting linear system of delay differential equations and Volterra equations:

$$
\begin{aligned}
\dot{U}_1(t) &= f'(w_1^s) W_1(t-T) - U_1(t) + \gamma_1 U_2(R\sigma, t),\\
\dot{W}_1(t) &= -\hat{b}_3 W_1(t) + \gamma_3 W_2(R\sigma, t),\\
U_2(R\sigma, t) &= -\int_0^{\infty} K^u(t-s, R\sigma)[f'(w_1^s) W_1(s-T) + \gamma_1 U_2(R\sigma, s)]\, ds,\\
V_2(R, t) &= c_0 \int_0^{\infty} e^{-b_2(t-s)} U_1(s)\, ds - c_0 \int_0^{\infty} \sum_{n=0}^{\infty} e^{-B_n(t-s)} \psi_n(R)\\
&\quad \times \left[\int_0^s \sum_{m=1}^{\infty} \delta_m^u\, e^{-A_m(s-\tau)} [f'(w_1^s) W_1(\tau - T) + \gamma_1 U_2(R\sigma, \tau)] \langle \phi_m, \psi_n\rangle\, d\tau \right] ds,\\
W_2(R\sigma, t) &= \int_0^{\infty} K^w(t-s, R\sigma)[(\hat{b} - b_3) W_1(s) - \gamma_3 W_2(R\sigma, s)]\, ds\\
&\quad + k \int_0^{\infty} \sum_{n=1}^{\infty} \langle [D_3 \nabla^2 h - b_3 h], \xi_n\rangle \xi_n(R\sigma)\, e^{-C_n(t-s)} V_2(R, s)\, ds\\
&\quad - k \int_0^{\infty} \sum_{n=1}^{\infty} \langle h, \xi_n\rangle \xi_n(R\sigma)\, e^{-C_n(t-s)} \dot{V}_2(R, s)\, ds.
\end{aligned}
\tag{3.13}
$$

Using standard techniques for time varying systems, we seek a solution to the above system in the form of:

$$[U_1(t), W_1(t), U_2(R\sigma, t), V_2(R, t), W_2(R\sigma, t)]^T = [\hat{U}_1, \hat{W}_1, \hat{U}_2, \hat{V}_2, \hat{W}_2]^T e^{\lambda t}.$$

With this substitution the characteristic equation for (3.13) is given by the following determinant:

$$\det \begin{bmatrix} \lambda+1 & -f'(w_1^s)\,e^{-\lambda T} & -\gamma_1 & 0 & 0 \\ 0 & \lambda+\hat{b}_3 & 0 & 0 & -\gamma_3 \\ 0 & f'(w_1^s)\,e^{-\lambda T} I_1 & 1+\gamma_1 I_1 & 0 & 0 \\ -c_0 I_2 & c_0 f'(w_1^s)\,e^{-\lambda T} I_3 & c_0\gamma_1 I_3 & 1 & 0 \\ 0 & (b_3-\hat{b}_3) I_4 & 0 & -kI_5 & 1+\gamma_3 I_4 \end{bmatrix} = 0,$$

where the integrals I_j, $j = 1, \ldots, 5$ are appropriately defined below. As we are interested in studying the stability of the system, it suffices to consider only the eigenvalues λ with $\mathrm{Re}(\lambda) > \max\{-1, -b_2, -b_3\}$. With this restriction on the values λ the Lebesque dominated convergence theorem can be applied to the integrals below and the order of integration and summation can be interchanged to yield the following:

$$I_1 = \int_0^\infty \sum_{n=1}^\infty \delta_n^u \phi_n(R\sigma)\, e^{-(\lambda + A_n)s}\, ds = \sum_{n=1}^\infty \frac{\delta_n^u \phi_n(R\sigma)}{\lambda + A_n},$$

$$I_2 = \int_0^\infty e^{-(\lambda+b_2)s}\, ds = \frac{1}{\lambda + b_2},$$

$$I_3 = \int_0^\infty \sum_{n=0}^\infty e^{-(\lambda+B_n)s} \psi_n(R) \left[\int_0^s \sum_{m=1}^\infty \delta_m^u\, e^{-(\lambda+A_m)\tau} \langle \phi_m, \psi_n \rangle\, d\tau \right] ds$$

$$= \sum_{n=0}^\infty \sum_{m=1}^\infty \frac{\delta_m^u \psi_n(R) \langle \phi_m, \psi_n \rangle}{(\lambda + A_m)(\lambda + B_n)},$$

$$I_4 = \int_0^\infty \sum_{n=1}^\infty \delta_n^w \xi_n(R\sigma)\, e^{-(\lambda+C_n)s}\, ds = \sum_{n=1}^\infty \frac{\delta_n^w \xi_n(R\sigma)}{\lambda + C_n},$$

$$I_5 = \int_0^\infty \sum_{n=1}^\infty \langle [D_3\nabla^2 h - b_3 h], \xi_n \rangle \xi_n(R\sigma)\, e^{-(\lambda+C_n)s}\, ds$$

$$- \int_0^\infty \sum_{n=1}^\infty \langle h, \xi_n \rangle \xi_n(R\sigma) \lambda\, e^{-(\lambda+C_n)s}\, ds$$

$$= \sum_{n=1}^\infty \frac{\xi_n(R\sigma)}{\lambda + C_n} [\langle D_3\nabla^2 h, \xi_n \rangle - (\lambda + b_3)\langle h, \xi_n(r) \rangle].$$

Next we expand the determinant above to give the characteristic equation in the following form:

$$(\lambda+1)(1+\gamma_1 I_1)(\lambda + \hat{b}_3 + (\lambda + b_3)\gamma_3 I_4) - k\gamma_3 c_0 f'(w_1^s)\, e^{-\lambda T} I_5 [I_2 - (\lambda+1) I_3] = 0. \tag{3.14}$$

This expression is multiplied by $(\lambda + b_2)$, $(\lambda + A_1)$, and $(\lambda + C_1)$. With the infinite series representations computed above for the terms I_j, $j = 1, \ldots, 5$, we can define the following quantities:

$$P(\lambda) = (\lambda+1)(\lambda+b_2)\left(\lambda + A_1 + \gamma_1\delta_1^u\phi_1(R\sigma) + \gamma_1\sum_{n=2}^{\infty}\frac{\delta_n^u\phi_n(R\sigma)(\lambda+A_1)}{\lambda+A_n}\right)$$
$$\times\left((\lambda+\hat{b_3})(\lambda+C_1) + (\lambda+b_3)\left(\gamma_3\delta_1^w\xi_1(R\sigma) + \gamma_3\sum_{n=2}^{\infty}\frac{\delta_n^w\xi_n(R\sigma)(\lambda+C_1)}{\lambda+C_n}\right)\right) \tag{3.15}$$

and

$$Q(\lambda) = \gamma_3 c_0 f'(w_1^s)\left(k\xi_1(R\sigma)\varepsilon_1 + \sum_{n=2}^{\infty}\frac{k\xi_n(R\sigma)\varepsilon_n(\lambda+C_1)}{\lambda+C_n}\right)$$
$$\times\left[\lambda + A_1 - (\lambda+1)\left(\frac{3(\delta_1^u)^2}{R^3(1-\sigma^3)} + \sum_{n=1}^{\infty}\frac{\delta_1^u\psi_n(R)\langle\phi_1,\psi_n\rangle(\lambda+b_2)}{\lambda+B_n}\right.\right.$$
$$\left.\left. + \sum_{m=2}^{\infty}\frac{3(\delta_m^u)^2(\lambda+A_1)}{R^3(1-\sigma^3)(\lambda+A_m)} + \sum_{n=1}^{\infty}\sum_{m=2}^{\infty}\frac{\delta_m^u\psi_n(R)\langle\phi_m,\psi_n\rangle(\lambda+A_1)(\lambda+b_2)}{(\lambda+A_m)(\lambda+B_n)}\right)\right], \tag{3.16}$$

where we use the information that $\psi_0(R)\langle\phi_m,\psi_0\rangle = 3\delta_m^u/R^3(1-\sigma^3)$ and define:

$$\varepsilon_n = \langle D_3\nabla^2 h, \xi_n\rangle - (\lambda+b_3)\langle h, \xi_n\rangle.$$

With these definitions we can write the characteristic equation for (3.13) in the form:

$$P(\lambda) - Q(\lambda)\,e^{-\lambda T} = 0. \tag{3.17}$$

In order to compare the well mixed and diffusion models, (2.2) and (3.1), the kinetic parameters must be compared. Clearly the decay rates, b_i, and production rate, c_0, are the same for either model. In addition, the transfer rates in the first two equations of each model must match, which implies that $\alpha_1 = \gamma_1$ and $\alpha_3 = \gamma_3$. The volume of the first compartment is $4\pi R^3\sigma^3/3$, and the volume of the second compartment is $4\pi R^3(1-\sigma^3)/3$. Using this information and a mass balance between the related chemical species we see that the transfer rates for (2.2) can be related by $\alpha_4 = \sigma^3\alpha_1/(1-\sigma^3)$ and $\alpha_6 = \sigma^3\alpha_3/(1-\sigma^3)$. Finally, we must relate the parameters for transfer across the compartment boundaries in the diffusion model to the transfer rates in the well mixed model. By the law of conservation of mass and the divergence theorem we see that:

$$\dot{u}_2 V_2 = \alpha_4(u_1-u_2)V_2 = \iiint_{V_2} D_1\nabla^2 u_2\,dV = D_1\iint_{S_{R\sigma}}\nabla u_2\cdot n\,dS$$
$$= D_1\beta_1(u_1(t)-u_2(t))\iint_{S_{R\sigma}} dS = D_1\beta_1(u_1-u_2)4\pi R^2\sigma^2,$$

where $V_2 = 4\pi R^3(1-\sigma^3)/3$. Thus, $\alpha_4 = 3D_1\beta_1\sigma^2/R(1-\sigma^3)$. Similarly, we find $\alpha_6 = 3D_3\beta_3\sigma^2/R(1-\sigma^3)$ and $\kappa = 3D_3k/R(1-\sigma^3)$. These relationships among the parameters are used in both the theoretical comparisons of the models below and in the numerical results in the final section of the paper.

Proof of Theorem 3.1 The proof centers around a careful analysis of each of the terms given in (3.15) and (3.16). Since all of the terms in (3.15) were analyzed in

Busenberg and Mahaffy [4], only a summary of the pertinent results will be given.

Let the diffusivities D_i tend to infinity. As $\beta_i D_i$ and kD_3 remain finite, β_1, β_3, and k must tend to zero. Similar to Busenberg and Mahaffy [4] we can use the eigenvalue equations (3.3) and (3.9) and the Maclaurin series expansions for sine and cosine to show that for μ_1 and ω_1 small:

$$\begin{aligned} \beta_1 R &= \frac{\mu_1^2(1-\sigma^3)}{3\sigma^2} + O(\mu_1^4) \\ \beta_3 R &= \frac{\omega_1^2(1-\sigma^3)}{3\sigma^2} + O(\omega_1^4). \end{aligned} \tag{3.18}$$

With (3.18) used in (3.4) and (3.10), it is easy to see:

$$\lim_{\mu_1 \to 0} \delta_1^u \phi_1(R\sigma) = 1 \quad \text{and} \quad \lim_{\omega_1 \to 0} \delta_1^w \xi_1(R\sigma) = 1. \tag{3.19}$$

We use (3.18) and the mass balance relations to see that as $D_1, D_3 \to \infty$:

$$D_1\mu_1^2 \cong \frac{3D_1\beta_1 R\sigma^2}{(1-\sigma^3)} = \alpha_4 \quad \text{and} \quad D_3\omega_1^2 \cong \frac{3D_3\beta_3 R\sigma^2}{(1-\sigma^3)} = \alpha_6. \tag{3.20}$$

From (3.3) and (3.9) one can show that $\mu_n(1-\sigma) > (n-1)\pi$ and $\omega_n(1-\sigma) > (n-1)\pi$, which when combined with (3.4) and (3.10) yields:

$$|\delta_n^u \phi_n(R\sigma)| < \frac{2\beta_1 R(1-\sigma)}{(n-1)^2\pi^2} \quad \text{and} \quad |\delta_n^w \xi_n(R\sigma)| < \frac{2\beta_3 R(1-\sigma)}{(n-1)^2\pi^2}. \tag{3.21}$$

Assuming $\mathrm{Re}(\lambda) > \max\{-1, -b_2, -b_3\}$, we can use (3.21) to show:

$$\left| \sum_{n=2}^{\infty} \frac{\delta_n^u \phi_n(R\sigma)(\lambda + A_1)}{\lambda + A_n} \right| < \frac{\beta_1 R(1-\sigma)}{3}$$

and

$$\left| \sum_{n=2}^{\infty} \frac{\delta_n^w \xi_n(R\sigma)(\lambda + C_1)}{\lambda + C_n} \right| < \frac{\beta_3 R(1-\sigma)}{3}.$$

Thus, as β_1 and β_3 tend to zero, we find that the infinite sums in (3.15) vanish. We combine this information with the limiting formulae given by (3.19) and (3.20) to see that as the diffusivities, D_i, tend to infinity the limiting form of the expression (3.15) has the following form:

$$(\lambda+1)(\lambda+b_2)(\lambda+1+\alpha_4+\gamma_1)[(\lambda+\hat{b_3})(\lambda+b_3+\alpha_6)+(\lambda+b_3)\gamma_3]. \tag{3.22}$$

Next we study the terms of $Q(\lambda)$ in (3.16), which differ substantially from the ones studied in Busenberg and Mahaffy [4]. The inner product for ε_n is expanded and gives:

$$\xi_n(R\sigma)\varepsilon_n = \frac{2R(\sin[\omega_n(1-\sigma)] - \omega_n \cos[\omega_n(1-\sigma)])G(\lambda)}{\omega_n^3\sigma(1-\sigma)F_{\mathrm{nor}}(\omega_n)}, \tag{3.23}$$

where

$$\begin{aligned} G(\lambda) &= (\lambda+b_3)[\omega_n^3(1-\sigma)] + (\lambda+C_n) \\ &\quad \times [(2-\beta_3 R\sigma)(\omega_n \cos[\omega_n(1-\sigma)] - \sin[\omega_n(1-\sigma)]) - 2\omega_n\sigma]. \end{aligned}$$

As before the eigenvalue equation (3.9) can be applied to eliminate the trigonometric functions and yields:

$$\xi_n(R\sigma)\varepsilon_n = -2R\left(\frac{\sigma(\lambda+C_n)(\omega_n^2+1)(2-\beta_3 R\sigma)}{\omega_n^2(1-\sigma)G_{\text{nor}}(\omega_n,\beta_3)} + \frac{[(\lambda+b_3)(\omega_n^2(1-\sigma)-2\sigma)-2D_3\omega_n^2\sigma/R^2]H(n)}{\omega_n^2(1-\sigma)G_{\text{nor}}(\omega_n,\beta_3)}\right), \tag{3.24}$$

where

$$H(n) = (-1)^{n-1}\sqrt{(\omega_n^2+1)(\omega_n^2\sigma^2+1+2\beta_3 R\sigma+\beta_3^2R^2\sigma^2)}. \tag{3.25}$$

When $n=1$, $\omega_1(1-\sigma)$ is small and we can apply the Maclaurin series expansions for sine and cosine to (3.23) to give:

$$\xi_1(R\sigma)\varepsilon_1 = \frac{3D_3}{R(1-\sigma^3)} + O(\omega_1^2). \tag{3.26}$$

For $n \geqslant 2$, (3.24) can be used for our analysis. For R and σ fixed we consider D_3 large which implies β_3 is small. Ignoring the terms with β_3, we find from (3.25) that:

$$H(n) \cong (-1)^{n-1}\sqrt{(\omega_n^2+1)(\omega_n^2\sigma^2+1)} \cong (-1)^{n-1}\left(\omega_n^2\sigma+\frac{\sigma}{2}+\frac{1}{2\sigma}\right)+O(1/\omega_n^2).$$

Again ignoring the terms with β_3 and substituting the above expression for $H(n)$, we find:

$$\xi_n(R\sigma)\varepsilon_n \cong 2R(-1)^{n-1}(\lambda+b_3)\frac{(\omega_n^2(1-\sigma)-\sigma)\left(\omega_n^2\sigma^2+\dfrac{\sigma^2+1}{2\sigma}\right)}{\omega_n^4(1-\sigma)^2(\omega_n^2\sigma^2+\sigma^2+\sigma+1)}$$
$$-4R\sigma(\lambda+C_n)\frac{\left((\omega_n^2+1)+(-1)^{n-1}\left(\omega_n^2\sigma+\dfrac{\sigma^2+1}{2\sigma}\right)\right)}{\omega_n^4(1-\sigma)^2(\omega_n^2\sigma^2+\sigma^2+\sigma+1)}.$$

It is easily verified that:

$$\frac{\left(\omega_n^2\sigma^2+\dfrac{\sigma^2+1}{2\sigma}\right)}{(\omega_n^2\sigma^2+\sigma^2+\sigma+1)} < \frac{1}{\sigma} \quad \text{and} \quad \frac{\left(\omega_n^2(1+\sigma)+1+\dfrac{\sigma^2+1}{2\sigma}\right)}{(\omega_n^2\sigma^2+\sigma^2+\sigma+1)} < \frac{1+\sigma}{\sigma^2}.$$

The eigenvalue equation (3.9) gives the inequality:

$$\omega_n > \frac{(n-1)\pi}{1-\sigma},$$

so with the above approximations we see that:

$$|\xi_n(R\sigma)\varepsilon_n| \leqslant \frac{2R(1-\sigma)}{\sigma(n-1)^2\pi^2}\left[|\lambda+b_3|+\frac{2(1-\sigma^2)|\lambda+C_n|}{(n-1)^2\pi^2}\right], \qquad n \geqslant 2.$$

For $\text{Re}(\lambda) > -b_3$, $|\lambda+C_1|/|\lambda+C_n| < 1$. With this we can form the following bound:

$$\left|\sum_{n=2}^{\infty}\frac{\xi_n(R\sigma)\varepsilon_n(\lambda+C_1)}{\lambda+C_n}\right| \leqslant \sum_{n=2}^{\infty}\frac{|\xi_n(R\sigma)\varepsilon_n||\lambda+C_1|}{|\lambda+C_n|} < M_1|\lambda+b_3|+M_2|\lambda+C_1|, \tag{3.27}$$

where

$$M_1 = \frac{2R(1-\sigma)}{\sigma\pi^2} \sum_{n=1}^{\infty} \frac{1}{n^2}$$

and

$$M_2 = \frac{4R(1-\sigma)(1-\sigma^2)}{\sigma\pi^4} \sum_{n=1}^{\infty} \frac{1}{n^4}.$$

From (3.24) and the balance laws computed before the beginning of this proof we obtain:

$$\lim_{D_3 \to \infty} k\xi_1(R\sigma)\varepsilon_1 = \lim_{D_3 \to \infty} \left(\frac{3kD_3}{R(1-\sigma^3)} + O(\omega_1^2) \right) = \kappa. \tag{3.28}$$

Thus, with (3.27) and (3.28) and provided the imaginary part of λ is bounded, we find:

$$\lim_{D_3 \to \infty} \left(k\xi_1(R\sigma)\varepsilon_1 + \sum_{n=2}^{\infty} \frac{k\xi_n(R\sigma)\varepsilon_n(\lambda + C_1)}{\lambda + C_n} \right) = \kappa, \tag{3.29}$$

where κ is a fixed parameter from the well mixed model. (Recall: $k \to 0$ as $D_3 \to \infty$.)

It remains to analyze the last factor in (3.16). We must show that the infinite sums in this factor tend to zero as the D_is tend to infinity and the term with δ_1^u tends to one. As stated before, $\delta_m^u \psi_0(R)\langle \phi_m, \psi_0 \rangle = 3(\delta_m^u)^2/R^3(1-\sigma^3)$, which from the expression for δ_m^u gives:

$$\begin{aligned} \frac{3(\delta_m^u)^2}{R^3(1-\sigma^3)} &= \frac{6\beta_1^2 R^2\sigma^2(\sin[\mu_m(1-\sigma)] - \mu_m \cos[\mu_m(1-\sigma)])^2}{\mu^3(1-\sigma^3)F_{\text{nor}}(\mu_m, \beta_1)} \\ &= \frac{6\beta_1^2 R^2\sigma^4(1+\mu_m^2)}{\mu^2(1-\sigma^3)G_{\text{nor}}(\mu_m, \beta_1)}. \end{aligned} \tag{3.30}$$

By using the expressions (3.18) derived from the Maclaurin series expansions in (3.30), we can see that $3(\delta_1^u)^2/R^3(1-\sigma^3) = 1 + O(\mu_1^2)$. By expanding $G_{\text{nor}}(\mu_m, \beta_1)$ and using $\mu_m(1-\sigma) \geqslant (m-1)\pi$, we can show:

$$\begin{aligned} \left| \sum_{m=2}^{\infty} \frac{3(\delta_m^u)^2(\lambda + A_1)}{R^3(1-\sigma^3)(\lambda + A_m)} \right| &\leqslant \sum_{m=2}^{\infty} \frac{6\beta_1^2 R^2\sigma^4(1+\mu_m^2)|\lambda + A_1|}{\mu_m^2(1-\sigma^3)G_{\text{nor}}(\mu_m, \beta_1)|\lambda + A_m|} \\ &\leqslant \frac{6\beta_1^2 R^2\sigma^2(1-\sigma)^2}{\pi^4(1+\sigma+\sigma^2)} \sum_{m=1}^{\infty} \frac{1}{m^4}. \end{aligned}$$

Clearly, this expression tends to zero as $\beta_1 \to 0$.

The next step is to examine $\delta_m^u \psi_n(R)\langle \phi_m, \psi_n \rangle$. By expanding the inner product we can show:

$$\delta_m^u \psi_n(R)\langle \phi_m, \psi_n \rangle = \frac{4\beta_1^2 R^2\sigma^4 \nu_n^2(\mu_m^2 + 1)(-1)^n \sqrt{(\nu_n^2 + 1)(\nu_n^2\sigma^2 + 1)}}{(\mu_m^2 - \nu_n^2)G_{\text{nor}}(\mu_m, \beta_1)G_{\text{nor}}(\nu_n, 0)}. \tag{3.31}$$

As we have noted before, $\mu_m(1-\sigma) \to (m-1)\pi$, and $\nu_n(1-\sigma) \to n\pi$. To analyze the term in the denominator, $\mu^2 - \nu^2$, suppose $\mu_m(1-\sigma) \cong k\pi$ and $\nu_n(1-\sigma) \cong k\pi$. Using the formulae (3.3) and (3.7), we perform a Taylor's series expansion about $k\pi$. It can be shown that $\mu_m(1-\sigma) = k\pi + (1-\sigma)^2/\sigma k\pi + \beta_1 R(1-\sigma)/k\pi + O(1/k^3\pi^3)$ and $\nu_n(1-\sigma) = k\pi + (1-\sigma)^2/\sigma k\pi + O(1/k^3\pi^3)$ for $\beta_1 R$ sufficiently small. Thus, $(\mu_m^2 - \nu_n^2)(1-\sigma)^2 = 2\beta_1 R(1-\sigma) + O(1/k^2\pi^2)$, when $m - 1 = n = k$. As this case gives the smallest denominator, we

see that $|\mu_m^2 - \nu_n^2| \geq 2\beta_1 R/(1-\sigma) > 2\beta_1 R$, for $m \geq 2$ and $n \geq 1$. With the above approximation and (3.31) we see that:

$$|\delta_m^u \psi_n(R)\langle\phi_m, \psi_n\rangle| < \frac{4\beta_1^2 R^2 \sigma^4 \nu_n^2 (\mu_m^2+1)\sqrt{(\nu_n^2+1)(\nu_n^2\sigma^2+1)}}{2\beta_1 R G_{\text{nor}}(\mu_m, \beta_1) G_{\text{nor}}(\nu_n, 0)}$$
$$\leq \frac{2\beta_1 R}{\mu_m^2(1-\sigma)^2} \leq \frac{2\beta_1 R}{(m-1)^2\pi^2}.$$

If we assume that $\text{Re}(\lambda) > \max\{-1, -b_2\}$, then:

$$|\lambda + A_m| > D_1 \mu_m^2/R^2 > D_1 \left(\frac{(m-1)\pi}{1-\sigma}\right)^2, \qquad m \geq 2,$$

$$|\lambda + B_n| > D_2 \nu_n^2/R^2 > D_2 \left(\frac{n\pi}{1-\sigma}\right)^2, \qquad n \geq 1.$$

We apply this to the double sum in (3.16) and find:

$$\left|\sum_{n=1}^{\infty}\sum_{m=2}^{\infty} \frac{\delta_m^u \psi(R)\langle\phi_m, \psi_n\rangle(\lambda + A_1)(\lambda + b_2)}{(\lambda + A_m)(\lambda + B_n)}\right|$$
$$\leq |\lambda + A_1||\lambda + b_2| \sum_{n=1}^{\infty}\sum_{m=2}^{\infty} \frac{|\delta_m^u \psi_n(R)\langle\phi_m, \psi_n\rangle|}{|\lambda + A_m||\lambda + B_n|}$$
$$\leq |\lambda + A_1||\lambda + b_2| \frac{2\beta_1 R(1-\sigma)^4}{D_1 D_2 \pi^6} \sum_{n=1}^{\infty} \frac{1}{n^2} \sum_{m=2}^{\infty} \frac{1}{(m-1)^4}.$$

Assuming that the imaginary part of λ is bounded, we can easily see that the above expression tends to zero as $D_1, D_2 \to \infty$. A similar argument shows that the remaining infinite sum in (3.16) also tends to zero as $D_2 \to \infty$.

To complete the analysis of (3.16), assume $D_i \to \infty$, $i = 1, 2, 3$, and that $\text{Re}(\lambda) > \max\{-1, -b_2, -b_3\}$. With the above results showing that the infinite sums vanish, (3.20) and (3.28) demonstrate the following:

$$\lim_{D_i \to \infty} Q(\lambda) = c_0 \kappa \gamma_3 \alpha_4 f'(w_1^s). \tag{3.32}$$

Using truncated Maclaurin series expansions with the mass balance relations, we can follow the steady state calculations in the Appendix and demonstrate that as $D_i \to \infty$, the steady state, w_1^s, of the diffusion model approaches the steady state, $\bar{w}_1$, of the well mixed model. From the limiting forms of Eqs. (3.15) and (3.16) given by (3.22) and (3.32), and as $\gamma_i = \alpha_i$, we see that for large diffusivities the characteristic equation of the diffusion model approaches the characteristic equation (2.3) of the well mixed model. The conclusion of Theorem 3.1 follows. This shows that the qualitative behavior of (2.1) with high diffusivities D_i, $i = 1, 2, 3$, should be similar to the behavior of the well mixed model (2.2).

For certain parameter values the well mixed model has characteristic values with positive real parts. Thus (2.2) can exhibit an oscillatory behavior. The techniques developed in [12] can be used to determine exactly where the Hopf bifurcation for (2.2) occurs. It follows from Theorem 3.1 that if the diffusivities D_i are sufficiently high then (3.1) can exhibit oscillatory behavior or undergo a Hopf bifurcation to small amplitude periodic solutions.

4 Bifurcation curves

The characteristic equation given by (3.17) is used to determine the critical delay, T, where a Hopf bifurcation occurs with respect to one of the parameters. The method of evaluating the critical delay uses a modification of the technique developed in [12] which handles the characteristic equation (2.3) of the well mixed model. The numerical scheme examines (3.17) for λ along the imaginary axis where the Hopf bifurcation occurs. The scheme relies on finding a value along the imaginary axis where the magnitude of $P(\lambda)$ is equal to the magnitude of $Q(\lambda)$. Subsequently, the arguments are adjusted by the delay T so that (3.17) is satisfied.

$P(\lambda)$ which is given by (3.15) has a leading power of λ equal to five, as is seen in (2.3) for the well mixed model. $Q(\lambda)$ acts more as a perturbation of the constant multiplying $e^{-\lambda T}$ in (2.3). Thus, the magnitude of $P(\lambda)$ increases more rapidly than the magnitude of $Q(\lambda)$. If $|P(0)| \geq |Q(0)|$, then there can be no Hopf bifurcation and (3.1) is locally asymptotically stable. If $|P(0)| \leq |Q(0)|$, then a bisection technique can be used to find when $|P(iv^*)| = |Q(iv^*)|$ for some $v^* > 0$. The critical delay is given by:

$$T = \frac{\arg(P(iv^*)) - \arg(Q(iv^*))}{v^*}.$$

In Fig. 3 the bifurcation curve is computed with the diffusivities, D_i, $i = 1, 2, 3$, as the bifurcation parameters. The diffusivities are all taken to be equal in this computation. The dashed line shows the value where the Hopf bifurcation occurs for the corresponding well mixed model (2.2). The curve in Fig. 3 demonstrates that when the diffusivities are high the asymptotic behavior of the reaction diffusion model (3.1) is the same as the corresponding well mixed model (2.2), which agrees with the result of Theorem 3.1. As the diffusivities decrease, Fig. 3 shows that first the diffusivities act like an increased delay causing (3.1) to become more unstable. This agrees with our intuitive understanding that the diffusion process is increasing the time for the biochemical species to reach the point where their reactions occur. Figure 3 shows that as the diffusivities become very small, the processes of decay become dominant and (3.1) becomes stable.

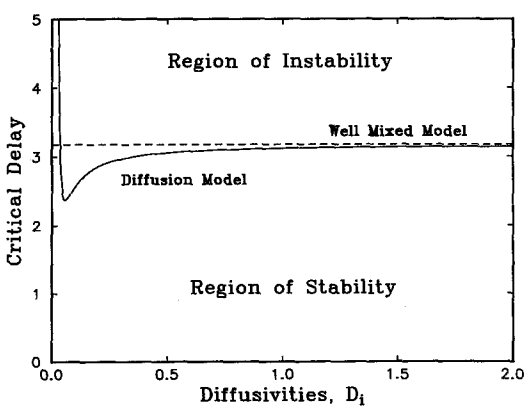

Fig. 3. Graph of the bifurcation curves for the models showing the critical delay, T, versus the diffusivities, D_i

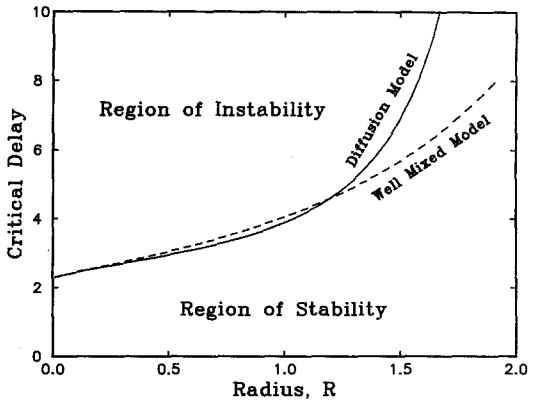

Fig. 4. Graph of the bifurcation curves for the models showing the critical delay, T, versus the cell radius, R

As the radius, R, of the cell becomes large, one expects that the biochemical species are diluted so that the probability of decay dominates the probability of reactions; hence, the models in (3.1) and (2.2) become asymptotically stable. Figure 4 demonstrates this result clearly. In addition, this figure shows that (3.1) becomes stable more rapidly than the well mixed model (2.2) with increasing R. This result is to be expected, as the increasing radius magnifies the delay effects of the diffusion process. The bifurcation curve in Fig. 4 parallels the results of Fig. 3. We observe the effects of diffusion first destabilizing the model (3.1) more than (2.2) with the bifurcation curve of the diffusion model dropping below the bifurcation curve of the well mixed model. Then as the decay processes begin to dominate, the bifurcation curve of the diffusion model rises more rapidly with increasing R.

The transfer rate constant κ in the well mixed model reflects the permeability of the cell membrane to the external nutrient and the concentration of the external nutrient. Figure 5 shows that as κ decreases, the models are increasingly stable. (Recall that κ and the transfer rate k are related by $\kappa = 3D_3k/R(1-\sigma^3)$.) This result is biologically the most significant, as increases in the external nutrient concentration could affect a cellular response by producing intracellular oscillations of the nutrient concentration. However, if the results of Fig. 4 and Fig. 5 are combined, it follows that a larger cell would require a higher

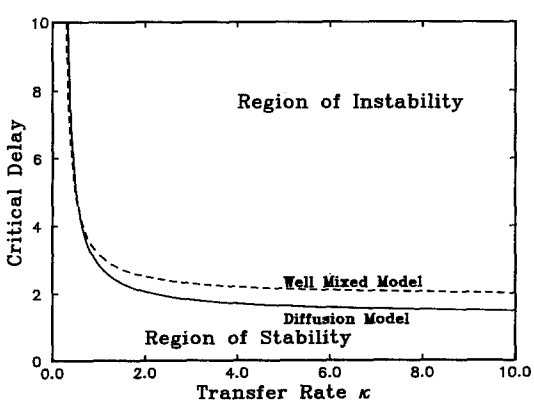

Fig. 5. Graph of the bifurcation curves for the models showing the critical delay, T, versus the transfer rate of the well mixed model, κ

concentration of external nutrient to produce oscillations. This demonstrates that smaller cells would be more sensitive to environmental changes.

5 Discussion

Active transport of a substance across the cellular membrane is an important biological process. We have considered a mathematical model of this process with genetic control by negative feedback. The model consists of two distinct compartments with diffusion allowed in the compartment representing the cytoplasm. The model also includes time delays for processes such as transcription and translation. The qualitative behavior of this model is examined for several of the parameters assuming radial symmetry.

This model shows that the techniques of Busenberg and Mahaffy [4, 5] can be extended to more complicated systems. For a certain class of models these methods can reduce a system of partial differential equations with delays to a system of delay differential equations and linear Volterra equations which no longer have any spatial dependence. This allows analysis of the system using standard methods for time varying systems. In particular, local analysis can be used to find where a Hopf bifurcation occurs. This analysis provides information on parameter ranges where the mathematical model changes from a region of stability to one where the model exhibits oscillations. An adaptation of the techniques developed in Mahaffy [12] allows the construction of bifurcation curves which can be interpreted in terms of their biological parameters.

As expected, the result of Theorem 3.1 shows that when the diffusivities are large, the qualitative behavior of the mathematical model with diffusion approaches that of a corresponding well mixed model. More significantly, the technique for proving the result produces a characteristic equation which can be analyzed in more detail. The results of Mahaffy et al. [13] which establish stability results for this model show that detailed analysis can be significantly more complicated. However, the characteristic equation is readily analyzed numerically and provides several interesting results.

As the diffusivities vary, the bifurcation curve of Fig. 3 shows several distinct behaviors. As noted above, high diffusivities give a qualitative behavior similar to that of the corresponding well mixed model. As the diffusivities are decreased, the bifurcation curve produces a range of decreasing stability which corresponds to the intuitive idea that diffusion acts as a time delay. However, when the diffusivities become sufficiently small, the biochemical species are unable to diffuse sufficiently through the cell before they decay, which results in increasing stability. Mahaffy et al. [13] prove that for diffusivities below some critical value, (3.1) is stable independent of the transcription-translation delay. The results shown in Fig. 3 are very similar to the results of Busenberg and Mahaffy [3, 5] for a simpler model with autorepression. This suggests a generic property for the diffusivity coefficient in this type of model where it destabilizes the model up to a point by acting like a time delay, then stabilizes the model as decay processes begin dominating the transport by diffusion.

As the cell grows, the radius increases and allows more time for the biochemical species to decay before they reach either the cellular membrane or the nucleus. This is very similar to the situation described above where the smaller diffusion rates prevent the reactions necessary for oscillatory behavior. It can be proved that there is a critical radius above which (3.1) is asymptotically

stable [13]. Figure 4 shows that the region of stability increases monotonically with increasing R; however, Busenberg and Mahaffy [3] showed in a related model that this is not always the case. The general shape of Fig. 4 agrees with the results of Busenberg and Mahaffy [3, 5] for the simpler autorepression model. Again this indicates that for the most part increasing cell size has a stabilizing effect on this class of cell models.

Our final result concerns the behavior of the model (3.1) in response to changes in extracellular concentration of the nutrient. Biologically, this could have important implications. The delay of the model is fixed, so if one follows a horizontal path in the bifurcation diagram of Fig. 5, then as the concentration of the external nutrient increases from zero, the model could pass from a region of stability to a region where the model displays oscillatory behavior. This oscillatory behavior could result in a signal for the cell to modify its response. If the external nutrient were a morphogen, then the increased concentration and resulting instability could cause the cell to undergo a developmental change or morphogensis.

A Appendix

In this section a summary of the calculations necessary for obtaining the steady state solution for the reaction-diffusion model is presented. To find the steady state solution, the time derivatives in (3.1) are set equal to zero. The result is a system of two algebraic equations and three boundary value problems which are given by the following:

$$\begin{aligned} f(w_1^s) &= u_1^s(1+\gamma_1) - \gamma_1 u_2^s(R\sigma), \\ (\gamma_3 + \hat{b_3})w_1^s &= \gamma_3 w_2^s(R\sigma), \\ D_1\nabla^2 u_2^s - u_2^s &= 0, \\ D_2\nabla^2 v_2^s - b_2 v_2^s &= -c_0 u_2^s, \\ D_3\nabla^2 w_2^s - b_3 w_2^s &= 0, \end{aligned} \tag{A.1}$$

with boundary conditions

$$\begin{aligned} \frac{du_2^s(R\sigma)}{dr} &= \beta_1(u_2^s(R\sigma) - u_1^s), & \frac{du_2^s(R)}{dr} &= 0, \\ \frac{dv_2^s(R\sigma)}{dr} &= 0, & \frac{dv_2^s(R)}{dr} &= 0, \\ \frac{dw_2^s(R\sigma)}{dr} &= \beta_3(w_2^s(R\sigma) - w_1^s), & \frac{dw_2^s(R)}{dr} &= kv_2^s(R), \end{aligned}$$

where

$$\nabla^2 = \frac{1}{r^2}\frac{d}{dr}\left(r^2\frac{d}{dr}\right).$$

Define $\delta_i^2 = b_i/D_i$, $i = 1, 2, 3$ $(b = 1)$, then solve for u_2^s, v_2^s, and w_2^s with the boundary conditions.

The equation for u_2^s with its boundary conditions is found to have the following solution:

$$u_2^s(R\sigma) = \frac{A_1}{R\sigma}\left(\cosh[\delta_1 R(1-\sigma)] - \frac{1}{\delta_1 R}\sinh[\delta_1 R(1-\sigma)]\right) \equiv q_1 A_1, \quad \text{(A.2)}$$

for A_1 defined below and q_1 an appropriately defined constant. Let $a_1 = R\delta_1(1+\beta_1 R\sigma - \sigma)$ and $a_2 = (R^2\sigma\delta_1 - 1 - \beta_1 R\sigma)$, then the constant A_1 is given by:

$$A_1 = \frac{\beta_1 R^3\sigma^2\delta_1 u_1^s}{a_1\cosh[\delta_1 R(1-\sigma)] + a_2\sinh[\delta_1 R(1-\sigma)]} \equiv q_2 u_1^s, \quad \text{(A.3)}$$

where q_2 is an appropriately defined constant.

Let $v_{2h}^s(r) = (1/r)(B_1\cosh[\delta_2(R-r)] + B_2\sinh[\delta_2(R-r)])$, then with the variation of constants formula and the boundary conditions, the following equations for B_1 and B_2 can be obtained:

$$B_1(\cosh[\delta_2 R(1-\sigma)] + \delta_2 R\sigma\sinh[\delta_2 R(1-\sigma)]) = -B_2(\sinh[\delta_2 R(1-\sigma)] + \delta_2 R\sigma\cosh[\delta_2 R(1-\sigma)])$$

and

$$B_1 + \delta_2 R B_2 = \frac{c_0 A_1}{D_2\delta_2}\left(\int_{R\sigma}^{R}\left(\frac{1}{\delta_1 R}\sinh[\delta_1(R-r)] - \cosh[\delta_1(R-r)]\right)\sinh[\delta_2(R-r)]\,dr + \delta_2 R\int_{R\sigma}^{R}\left(\cosh[\delta_1(R-r)] - \frac{1}{\delta_1 R}\sinh[\delta_1(R-r)]\right)\cosh[\delta_2(R-r)]\,dr\right).$$

The two equations above can be rewritten as:

$$B_1 = -q_3 B_2 \quad \text{(A.4)}$$

and

$$B_1 + \delta_2 R B_2 = -q_4 A_1, \quad \text{(A.5)}$$

by defining q_3 and q_4 appropriately.

Let $w_2^s(r) = (1/r)(C_1\cosh[\delta_3(R-r)] + C_2\sinh[\delta_3(R-r)])$, then the boundary conditions yield the following equations:

$$((1+\beta_3 R\sigma)\cosh[\delta_3 R(1-\sigma)] + \delta_3 R\sigma\sinh[\delta_3 R(1-\sigma)])C_1$$

$$((1+\beta_3 R\sigma)\sinh[\delta_3 R(1-\sigma)] + \delta_3 R\sigma\cosh[\delta_3 R(1-\sigma)])C_2 = \beta_3 R^2\sigma^2 w_1^s$$

and

$$C_1 + \delta_3 R C_2 = -kRB_1 + \frac{c_0 k A_1}{D_2\delta_2}\int_{R\sigma}^{R}\left(R\cosh[\delta_1(R-r)] - \frac{1}{\delta_1}\sinh[\delta_1(R-r)]\right) \times \sinh[\delta_2(R-r)]\,dr.$$

To simplify the notation we write the first of these equations as follows:

$$C_1 + p_5 C_2 = q_5 w_1^s, \quad \text{(A.6)}$$

and the second equation can be defined:

$$C_1 + \delta_3 RC_2 = -kRB_1 + q_6 A_1, \tag{A.7}$$

for the appropriately defined p_5, q_5, and q_6. The solution for w_2^s substituted into the equation for dw_1^s/dr yields:

$$R\sigma(\gamma_3 + \hat{b_3})w_1^s = \gamma_3(C_1 \cosh[\delta_3 R(1-\sigma)] + C_2 \sinh[\delta_3 R(1-\sigma)]),$$

which can be written as:

$$C_1 + p_7 C_2 = q_7 w_1^s, \tag{A.8}$$

for p_7 and q_7 appropriately defined.

With some algebraic manipulations Eqs. (A.2–8) can be combined into a single nonlinear equation in w_1^s as given below:

$$f(w_1^s) = \left(\frac{(1+\gamma_1 - \gamma_1 q_1 q_2)(q_3 - \delta_2 R)[p_7 q_5 - p_5 q_7 + \delta_3 R(q_7 - q_5)]}{q_2(q_3 q_6 + kRq_3 q_4 - \delta_2 Rq_6)(p_7 - p_5)} \right) w_1^s.$$

If the coefficient of w_1^s on the right hand side of the above equation is positive, then from the definition of the function f there is a unique solution to this nonlinear equation which can be readily found by Newton's method. The positivity of the coefficient on the right hand side has not been proved. From the equations above it is clear that once one has computed w_1^s, then it is easy to obtain the complete steady state solution for (3.1).

References

1. Banks, H. T.: Modeling and Control in the Biomedical Sciences. (Lect. Notes Biomath., Vol. 6) Berlin Heidelberg New York: Springer 1975
2. Banks, H. T., Mahaffy, J. M.: Mathematical models of protein synthesis. (Tech. Rep., Division of Applied Mathematics) Providence, RI: Lefschetz Center for Dynamical Systems 1979
3. Busenberg, S. N., Mahaffy, J. M.: A compartmental reaction diffusion cell cycle model. Computer. Math. Appl. **18**, 883–892 (1989)
4. Busenberg, S. N., Mahaffy, J. M.: The effects of dimension and size for a compartmental model of repression. SIAM J. Appl. Math. **48**, 882–903 (1988)
5. Busenberg, S. N., Mahaffy, J. M.: Interaction of spatial diffusion and delays in models of genetic control by repression. J. Math. Biol. **22**, 313–333 (1985)
6. Goodwin, B. C.: Oscillatory behavior of enzymatic control processes. Adv. Enzyme Regul. **3**, 425–439 (1965).
7. Harter, J. R., Molony, J., Sievers R.: A reaction diffusion model with extracellular control. (Tech. Rep., San Diego State University) San Diego, CA: Department of Mathematical Sciences 1987
8. Klebba, P. E., MacIntosh, M. A., Neilands, J. B.: Kinetics of biosynthesis of iron-regulated membrane proteins in *Escherichi coli*. J. Bacteriol. **149**, 880–888 (1982).
9. Lundrigan, M. D., Kadner, R. J.: Altered cobalamin metabolism in *Escherichia coli btuR* mutants affects *btuB* gene regulation. J. Bacteriol. **171**, 154–161 (1989).
10. Lundrigan, M. D., Kadner, R. J.: Nucleotide sequence of the gene for the ferrienterochelin receptor FepA in *Escherichia coli*. J. Biol. Chem. **261**, 10797–10801 (1986).
11. MacIntosh, M. A., Earhart, C. F.: Coordinate regulation by iron of the synthesis of phenolate compounds and three outer membrane proteins in *Escherichia coli*. J. Bacteriol. **131**, 331–339 (1977).
12. Mahaffy, J. M.: A test for stability of linear differential delay equations. Q. Appl. Math. **40**, 193–202 (1982).

13. Mahaffy, J. M., Jorgensen, D. A., Vanderheyden, R. L.: Stability results for a model of repression with external control. Q. Appl. Math. (to appear)
14. Mahaffy, J. M., Pao, C. V.: Models of genetic control by repression with time delays and spatial effects. J. Math. Biol. **20**, 39–58 (1984)
15. Neilands, J. B.: Microbial envelope proteins related to iron. Annv. Rev. Microbiol. **36**, 285–309 (1982)
16. Neilands, J. B.: Microbial iron compounds. Annv. Rev. Biochem. **50**, 715–731 (1981).
17. Neville, M. M., Suskind, S. R., Roseman, S.: A derepressible active transport system for glucose in *Neurospora crassa*. J. Biol. Chem. **246**, 1294–1301 (1971)
18. Othmer, H. G.: The qualitative dynamics of a class of biochemical control circuits. J. Math Biol. **3**, 53–78 (1976)
19. Ramos, J., Szkutnicka, K., Cirillo, V. P.: Relationship between low- and high-affinity glucose transport systems of *Saccharomyces cerevisiae*. J. Bacteriol. **170**, 5375–5377 (1988).
20. Rapp, P. E.: Mathematical techniques for the study of oscillations in biochemical control loops. Bull. Inst. Math. Appl. **12**, 11–20 (1976)
21. Roseman, S.: The transport of carbohydrates by a bacterial phosphotransferase system. J. Gen. Physiol. **54**, 138s–184s (1968)
22. Rosenberg, H., Gerdes, R. G., Chegwidden, K.: Two systems for the uptake of phosphate in *Escherichia coli*. J. Bacteriol. **131**, 505–511 (1977)
23. Surin, B. P., Rosenberg, H., Cox, G. B.: Phosphate-specific transport system of *Escherichia coli*: Nucleotide sequence and gene-polypeptide relationships. J. Bacteriol. **161**, 189–198 (1985)
24. Tyson, J. J., Othmer, H. G.: The dynamics of feedback control circuits in biochemical pathways. In: Rosen, R., Snell, F. M. (eds.) Prog. in Theor. Biol. New York: Academic Press 1978